

Adsorption of polyelectrolytes on charged microscopically patterned surfaces

Amin Bakhshandeh^{1,2, a)} and Maximiliano Segala^{2, b)}

¹⁾Programa de Pós-Graduação em Física, Instituto de Física e Matemática, Universidade Federal de Pelotas, Caixa Postal 354, CEP 96010-900 Pelotas, RS, Brazil

²⁾Departamento de Físico-Química, Instituto de Química, Universidade Federal do Rio Grande do Sul, 591501-970, Porto Alegre, RS, Brazil

(Dated: 30 January 2020)

In the present study we have investigated, using Monte Carlo simulations (MC), the adsorption of polyelectrolytes on the charged nanopatterned surfaces. Different surface's patterns were considered and we noticed that the amount of adsorption is directly dependent on the size of the domains. Also in the case of checkerboard configuration it was observed that the polyelectrolytes are aligned along the diagonal of square domains.

I. INTRODUCTION

Polyelectrolytes are polymers which possess ionized groups in polar solvents. There are many systems which are considered as polyelectrolyte such as proteins, sulfonated and polyacrylic acids^{1,2}. They have a wide range of application from water treatment to tissue engineering^{3,4}. Normally the "Click" chemistry is used as a powerful and efficient method to synthesis these systems, in this method, by carbon-hetero bond formation, polymers can be synthesized⁵. As these components in polar solvents are charged, the electrostatic interaction in these systems plays an important role^{6,7}.

For example one of the important characteristics of polyelectrolytes is their extended chain, the main reason for this phenomena is Coulomb repulsion between charged segments^{8,9}, the extended chain of polyelectrolytes, in turn, leads to a bigger hydrodynamic volume⁹. As we mentioned earlier, these components have a very wide range of application, therefore it is of critical importance to have a deeper understanding of properties and behavior of these components. One way to evaluate the physical and chemical properties of materials is to study their adsorption to different surfaces. By doing so, it can shed light on some material's behavior within a chemical process. In biological systems, molecules should adsorb to the surface of the Enzyme catalysis on active sites, for this reason, the rate of reaction may depend on stability of the molecules on surfaces and also rate of adsorption and adherence. As a result, we can understand the importance of interaction of molecules with surfaces. There are many surfaces which gain charge inside polar solvents and since polyelectrolytes are charged the electrostatic interaction becomes significance for adsorption of polyelectrolytes on these surfaces.

At first glance, it may seem it is a simple problem because there are very primitive mean-field theories such as Debye-Hückel approximation to explain the behavior

of charged particles in aqueous solutions^{8,10-13}. However, it is well known that theoretical study of adsorption of charged particles on charged plates is not easy since mean-field approximation collapses to describe their behavior in high correlated regions^{8,13,14}. Nevertheless, there are some approximations using simple models such as one component plasma near a neutralizing background or some similar theories which work well in regions of high electrostatic correlations. The situation gets worse when surfaces are not homogeneously charged or some nanopatterns exist on them. However, always one of the best ways to study these systems is computational simulations¹⁵⁻²¹. There are many biological systems which their surfaces carry patterns, as an example, proteins can bind to some significant patterns of surfaces²²⁻²⁴. Nowadays, it is easy to create charged nano-structured surfaces, these periodic organized surfaces are found in nanostructures, magnetic storage media and nanowires²⁵⁻²⁸. The simulations of these systems are more complicated than the simulation of simple uniform charged surfaces. McNamara et al.²² studied adsorption of one polyelectrolyte on different patterned surfaces and approximated interaction between the charges on the surface and polyelectrolyte's monomers with a screened Coulomb interaction which obtained from the Debye-Hückel potential which is:

$$V(r) \propto \frac{e^{-k r}}{r}, \quad (1)$$

where k and r are inverse Debye length and interacting distance respectively. Eq. 1 is a mean-field potential and as a result in their simulations the effect of neighbors cell was not considered. One way to produce different patterns is to put point charges on surface²⁹, the drawback of this method is that, depending on the surface charge density and surface's size, one should put enough number of particles on the plate which this may lead to slow down the simulation. Recently, an efficient and robust method has been introduced to simulate nanopatterned charged surfaces inside an electrolyte solution³⁰. In the mentioned method, to deal with the long-range Coulomb interaction between the ions a modified 3d Ewald summation method was used³¹. The surfaces are considered as periodic charged sinusoidal patterns. The analytical

^{a)}Electronic mail: amin.bakhshandeh@ufrgs.br

^{b)}Electronic mail: maximiliano.segala@ufrgs.br

solution of the Poisson equation was evaluated in order to properly consider the effect of the nano-structured charged walls as an external potential. By using this method the adsorption of polyampholytes on these surfaces has been studied³².

In the present work we will use Monte Carlo simulations to study the adsorption of Polyelectrolytes on charged nano-patterns surfaces with the mentioned method. Our main aim is to observe the effect of charged patterns on adsorption of these macromolecules on nano-patterned surfaces.

The remainder of the paper is organized as follows.: In section II, we explain the model and the simulation details. In section III, we summarize our results. In section IV we conclude our work.

II. THE MODEL AND SIMULATION DETAILS

We model nano-patterned surface by a sinusoidal charge density, which mathematically can be described as follows³⁰:

$$\sigma(x, y) = \sigma_0 \sin(k_x x + \varphi_x) \sin(k_y y + \varphi_y), \quad (2)$$

where σ_0 is the amplitude, $\varphi_x = 0$ and $\varphi_y = \pi/2$ are the phases, $k_x = 2\pi n_x/L_x$, $k_y = 2\pi n_y/L_y$, with L_x and L_y periods of charge density oscillations in x and y directions, respectively, and $n_{x,y}$ are integers. By changing $n_{x,y}$ different patterns simply can be generated. We have plotted σ/σ_0 for four cases in Fig.1, where $\sigma_0 = 0.1 \text{ C/m}^2$.

It can be shown that the potential produced by this charge density can be written as³⁰

$$\Phi_1(\mathbf{r}) = \frac{2\pi\sigma_0}{\epsilon_w\alpha} \sin(k_x x + \varphi_x) \sin(k_y y + \varphi_y) e^{-\alpha|z|}, \quad (3)$$

where $\alpha = \sqrt{k_x^2 + k_y^2}$. We consider our system consisting of two flat surfaces of dimensions L_x and L_y , located at $z = -L/2$ and $z = L/2$ where $L = 300 \text{ \AA}$ enclosing the electrolyte solution. Also, we set $L_x = L_y = 200 \text{ \AA}$ to have a better statistic. The solvent is assumed to be an uniform dielectric of permittivity ϵ_w . The Bjerrum length is defined as $\lambda_B = e^2/k_B T \epsilon_w$ where e , k_B and T are the elementary charge, the Boltzmann constant and the absolute temperature, respectively. The Bjerrum length in current study is 7.2 \AA , a value for room temperature and $\epsilon_w = 80$.

The electrostatic potential produced by both surfaces is given by³⁰

$$\Phi(\mathbf{r}) = \frac{2\pi\sigma_0}{\epsilon_w\alpha} \sin(k_x x + \varphi_x) \sin(k_y y + \varphi_y) \left(e^{-\alpha|z+L/2|} + e^{-\alpha|z-L/2|} \right). \quad (4)$$

The dissociated 100 macromolecules between the surfaces are modeled with the primitive model. The

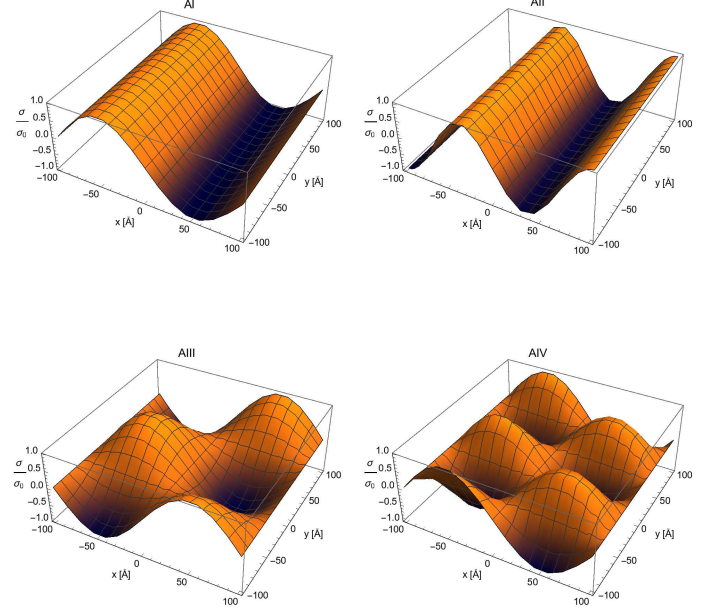


FIG. 1: Representation of σ/σ_0 against x and y direction for $\sigma_0 = 0.1 \text{ C/m}^2$ and $\varphi_x = \varphi_y = 0$. AI) $n_x = 1, n_y = 0$, AII) $n_x = 2, n_y = 0$, AIII) $n_x = 1, n_y = 1$, AIV) $n_x = 2, n_y = 2$.

monomers are modeled as hard spheres of radius 2 \AA , with centered negative charge $-e$. At first we consider polyelectrolytes which are composed of 18 monomers of charge $-e$. Since polyelectrolytes are overall charged, in order to make system neutral we add counterions to the systems. The adjacent monomers that compose a chain interact via a parabolic potential as $U_b(r) = A/2(r-r_0)^2$, where $A = 0.97 k_B T$, r is the distance between adjacent monomers and $r_0 = 5 \text{ \AA}$ ²¹. The simulations are performed using the Metropolis algorithm^{33,34}, with 5×10^7 MC steps for equilibration. Each sample is obtained with 300 trial movements per particle. The macromolecules can perform rotation move and head and tail monomer can be exchange at each MC movement. Moreover, monomers can have short displacements, which models vibration of segments²¹. Since the system has slab geometry we use a corrected 3D Ewald summation³¹. The total potential energy of the system composed of N hard sphere particles of charge q_i located at \mathbf{r}_i can be written as follows^{21,30}:

$$U = \sum_{\mathbf{k} \neq 0}^{\infty} \frac{2\pi}{\epsilon_w V |\mathbf{k}|^2} \exp\left[-\frac{|\mathbf{k}|^2}{4\kappa_e^2}\right] [A(\mathbf{k})^2 + B(\mathbf{k})^2] + \frac{2\pi}{\epsilon_w V} M_z^2 + \frac{1}{2} \sum_{i \neq j}^N q_i q_j \frac{\text{erfc}(\kappa_e |\mathbf{r}_i - \mathbf{r}_j|)}{\epsilon_w |\mathbf{r}_i - \mathbf{r}_j|} + \sum_{i=1}^N q_i \Phi(\mathbf{r}_i) + \sum' U_b(|\mathbf{r}_i - \mathbf{r}_j|), \quad (5)$$

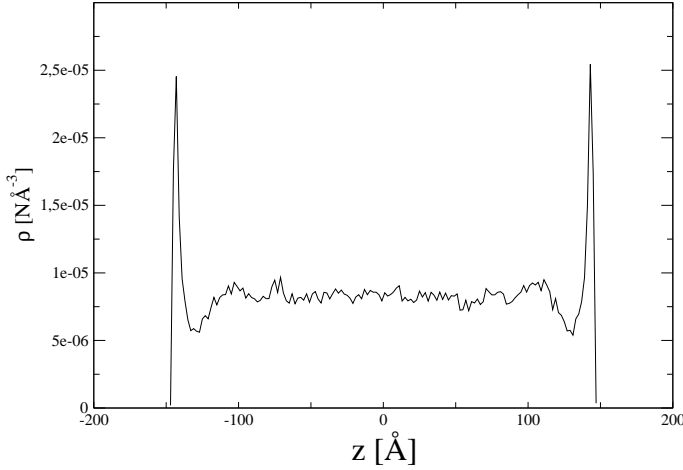


FIG. 2: Concentration profiles of polyelectrolytes (center of mass) for case of AI for polyelectrolytes with 18 monomers. $\sigma_0 = 0.1 \text{ C/m}^2$, $n_x = 1$ and $n_y = 0$

where

$$\begin{aligned} A(\mathbf{k}) &= \sum_{i=1}^N q_i \cos(\mathbf{k} \cdot \mathbf{r}_i) , \\ B(\mathbf{k}) &= - \sum_{i=1}^N q_i \sin(\mathbf{k} \cdot \mathbf{r}_i) , \\ M_z &= \sum_{i=1}^N q_i z_i , \end{aligned} \quad (6)$$

and $V = L_x \times L_y \times L_z$ is the volume of the main cell, while $L_z = 3L_x$. The \mathbf{k} vectors are defined as $\mathbf{k} = (\frac{2\pi}{L_x}n_x, \frac{2\pi}{L_y}n_y, \frac{2\pi}{L_z}n_z)$, where n 's are integers. Around 500 vectors are used in the calculation. The damping parameter is $\kappa_e = 5/L_x$. The restricted summation in the last sum in Eq. 5 is due to adjacent monomers in macromolecules.

III. RESULTS

As we discussed, for many chemical and physical process it is great of importance that molecules adsorb on the surfaces, as a result, it is interesting to study the effect of patterns on adsorption.

We put 100 polyelectrolytes in the cell in the presence of surfaces with different patterns. We have shown the density profile for $(n_x, n_y) = (1, 0)$ in Fig. 2.

As is seen in Fig. 2 there is high adsorption on surfaces. Since the charge of monomers is negative we expect to have more adsorption on domains with opposite charge of polyelectrolyte. We have plotted the density profile of monomers near the plate's surface for different (n_x, n_y) , which are (1, 0), (2, 0), (1, 1) and (3, 3) respectively. As is seen in Fig 3, all polymers are adsorbed in domains with

opposite charges, for the case of (1, 0), as the positive region is bigger the density peak is wider, however for $n_{x,y}$, (1, 1) the peaks become more sharper. The same phenomena is observed for (3, 3).

At this point, it is interesting to realize the geometrical configuration of adsorbed polyelectrolytes on different patterns. To this end, we use the separation distance between the first and the last monomer of each polyelectrolyte, by doing this we can obtain a picture of shape of polymer in different positions in the cell, especially near the plate. The mentioned distances are defined as follows:

$$\begin{aligned} \Delta x(z) &= \sqrt{\left\langle \frac{\sum_{i=1}^N (x_i^{\text{head}} - x_i^{\text{tail}})^2}{N(z)} \right\rangle}, \\ \Delta y(z) &= \sqrt{\left\langle \frac{\sum_{i=1}^N (y_i^{\text{head}} - y_i^{\text{tail}})^2}{N(z)} \right\rangle}, \\ \Delta z(z) &= \sqrt{\left\langle \frac{\sum_{i=1}^N (z_i^{\text{head}} - z_i^{\text{tail}})^2}{N(z)} \right\rangle}, \end{aligned} \quad (7)$$

where Δx , Δy and Δz are the rms components of the head-to-tail vector in x, y and z directions and $N(z)$ is the number of polyelectrolytes in each volume element in position z . We have plotted head to tail distances for cases AI, AII, AIII and AIV in Figs. 4 and 5.

As is seen in Fig. 4a for the case of $n_{x,y} = (1, 0)$ the Δz is more and less constant and both Δx and Δy components are high near the surface in comparison with bulk value. Nevertheless, Δy component is a little bit higher than Δx component, the reason is that polyelectrolytes prefer to extend along the positive region to have less repulsion from negative domains and have more attraction by positive domain.

For the case of $n_{x,y} = (2, 0)$ as is seen in Fig. 4b the Δx component decreases dramatically and Δy component increases. This also can be interpreted by using the Fig. 3, since the positive area on the plate decreases and the negative monomers do not like to be in contact with negative regions in this case polyelectrolytes adjust themselves in y direction, in order to be far away from negative regions on the plate. We have shown this configuration schematically in Fig. 6a

In next, we study the cases $n_{x,y} = (1, 1)$ and $n_{x,y} = (2, 2)$, as is observed in Fig. 5 for the case of $n_{x,y} = (1, 1)$ and $n_{x,y} = (2, 2)$, the values of Δx and Δy become equal near the plates, this is due to the fact that polyelectrolytes are aligned along the diagonal of domains, however for the case of AIV their values decreases, which this is because of smaller size of domain. In order to realize how the size of the domains and polyelectrolytes affect on the adsorption, we obtain $\Delta R = \sqrt{\Delta x^2 + \Delta y^2 + \Delta z^2}$ in bulk, by using MC simulation, for three different polyelectrolytes with number of segments 10, 18 and 25 respectively. ΔR for polyelectrolytes with 10, 18 and 25 is obtained 33, 63 and 80 Å. In next step, we implement

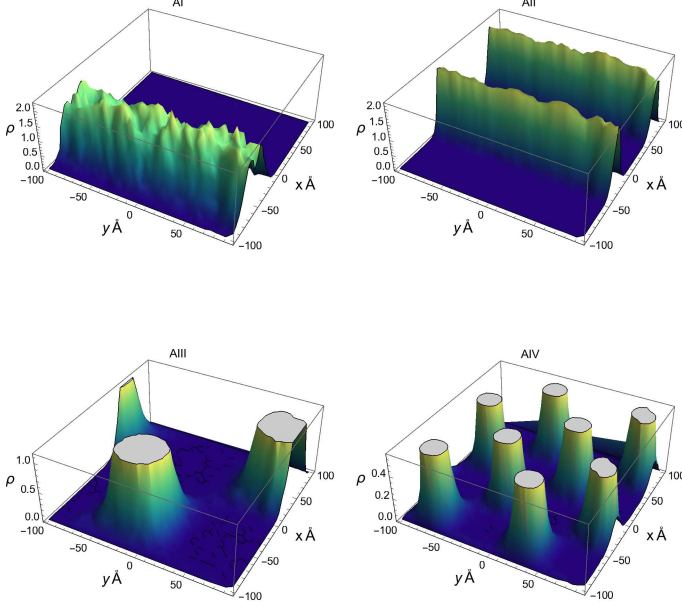


FIG. 3: Density profile of segments of polyelectrolytes with 18 monomer in a bin $\Delta z = 6$ Å at contact for AI) $n_x = 1$ and $n_y = 0$, AII) $n_x = 2$ and $n_y = 0$, AIII) $n_x = 1$ and $n_y = 1$, AIV) $n_x = 2$ and $n_y = 2$ respectively.

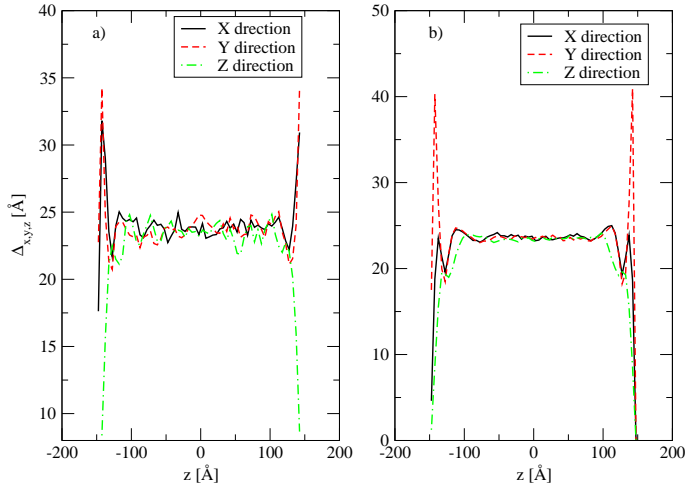


FIG. 4: Average distance of between head to tail of polyelectrolytes for component in x , y and z direction for a) case AI and b) AII.

MC simulation for different charge densities and patterns in the way that surface charge density gets scaled by $\sigma_0/n_x = 0.1$ C/m², also we put $n_x = n_y$ to create checkerboard configurations. The adsorption Γ can be

calculated by

$$\Gamma = \frac{1}{2} \int_{-L/2}^{L/2} (\rho(z) - \rho_b) dz, \quad (8)$$

where $\rho(z)$ and ρ_b are local and bulk density respectively. ρ_b is obtained by taking average of polyelectrolytes density at the middle of cell between $z = -25$ and $z = 25$ Å. As is seen in Fig. 7 when ΔR becomes comparable with domain's sides the adsorption starts to decrease, when the number of segments $N_{segments}$ is 10 this happens at $n_x = n_y = 4$ where domain's side, l , is 25 Å and when $N_{segments}$ is 18 this happens at $n_x = n_y = 3$ where $l = 33$ Å. We expect the same observation is seen for $N_{segments} = 25$ and decrease in Γ happens at $n_{x,y} = (2, 2)$, however we observe that not only decrease in $n_{x,y} = (2, 2)$ but also there is increment in $n_{x,y} = (3, 3)$. In Fig. 8 we have shown the density profiles of segments for two mentioned surface's configurations. As is seen for the case (3, 3) there is a wide peak at the center of each positive domain and for the case of (4, 4) the peaks become sharper which is due to repulsion force of other negative domains, however, between the peaks in diagonal directions, it is seen that there is a small density of segments which connect the peaks. This confirms the alignment of polymers in that direction, also the small magnitude of density in that regions suggests that the monomers stay in further distance from plates in comparison with other monomers. We show this configuration in Fig. 6b.

By looking at the Figs. 9 it is seen that the $\Delta_x = \Delta_y$ which shows the same conclusion about the polymer configuration. This shows that despite the repulsion of other negative neighbor domains the polymer can connect itself to other positive domains as is shown in Fig 6b. However, this adjustment of polymer costs energy because in the region between domains the monomers feel more repulsion and want to avoid that region. As a result, the segments get distance from surfaces. By decreasing the edge of the domains the repulsion force becomes too strong that this special shape does not help polymer to gain more negative energy, as a result the adsorption decreases as we expected. In the end, we studied the effect of the concentration of polyelectrolytes on adsorption. To this end, we consider a different number of polyelectrolytes with 10 segments inside the cell. We fixed the $\sigma_0 = 0.1$ C/m² and $n_{x,y} = (1, 0)$. As can be seen in Fig. 10 by increasing the polymer concentration the adsorption increases however very rapidly the adsorption stop increasing due to saturation of the surfaces.

IV. CONCLUSION

In the present work, we have studied the adsorption of poly- electrolytes to nano-patterned charged surfaces using a recent method for simulation of these kinds of systems³⁰. It is shown that all polyelectrolytes are adsorbed to domains with opposite charge and concentrated

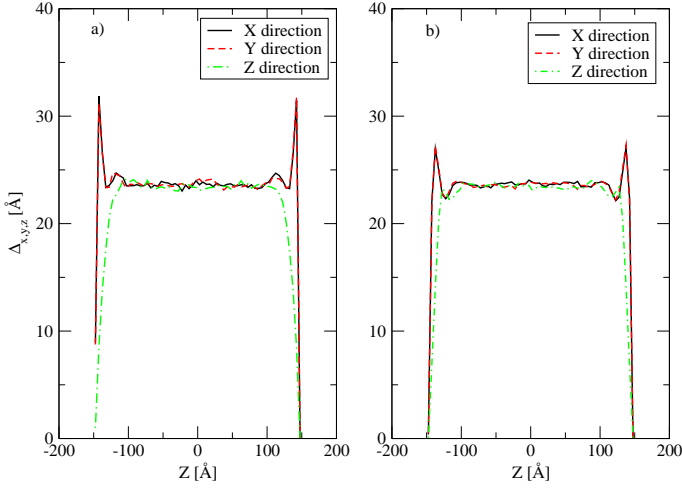


FIG. 5: Average distance of between head to tail of polyelectrolytes for component in x , y and z direction for a) case AIII and b) AIV.

at the center of the domains where there is higher charge density. By studying the average distance of head to tail of molecules we observed that the molecules prefer to become extended on the surface in direction of y for stripes configurations where the plate has transnational symmetry in that direction. Also, it was observed that the amount of adsorption may relate to the head to tail distance of molecule in bulk. For checkerboard configurations, when the edge of the domain becomes comparable with this significance distance (head to tail distance) the adsorption decreases for the same scaling variable which is σ_0/n_x . However for longer polyelectrolytes since they can have a bend configurations along the diagonal of square domains and still have some segments near the opposite charged domains, they can find a more stable configuration and reach to the center of others opposite neighbor charged domains via diagonal path and as a result it can be seen that adsorption increases by reducing the size of domains. However for $n_x = n_y = 4$ this configuration does not help to gain more attraction and stable configuration, as a result the adsorption reduces.

V. ACKNOWLEDGMENTS

This work was supported by CAPES under process number 88882.306664/2013-01.

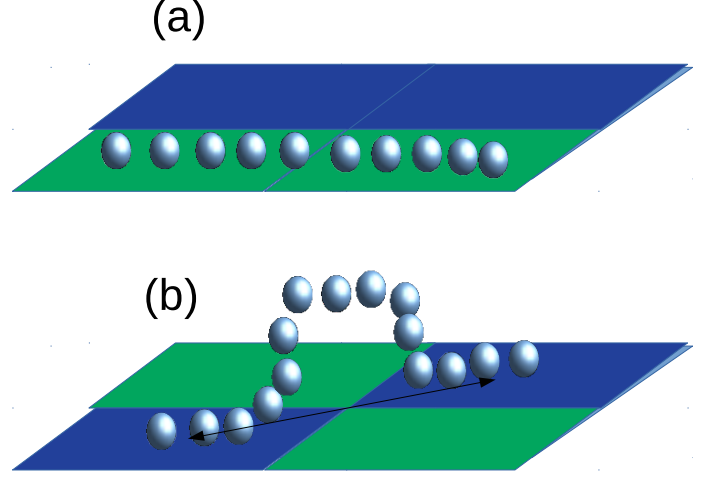


FIG. 6: The schematic representation of polyelectrolytes adsorbed on the charged patterned surfaces. a) Stripes configurations b) Checkerboard configurations. The long polyelectrolytes try to reach other opposite charged domains via diagonal of domains by getting distance from plate near the same charged domains.

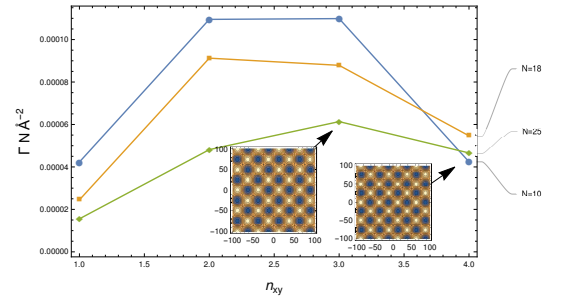


FIG. 7: The adsorption against n_x for polyelectrolytes with different number of segments $N_{segments} = 10, 18$ and 25 . The surface charge is normalized by $\sigma_0/n_x = 0.1 \text{ C/m}^2$. In all configurations $n_x = n_y$.

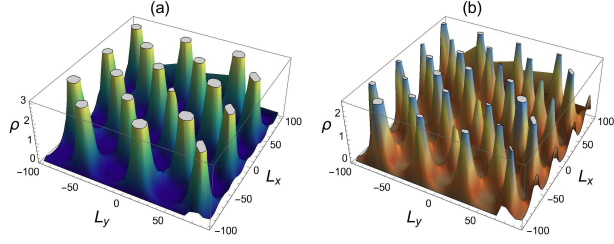


FIG. 8: Density profile of segments of polyelectrolytes in a bin $\Delta z = 6 \text{ \AA}$ at contact for polyelectrolyte with 25 segments. a) $n_x = 3, n_y = 3$, b) $n_x = 4$ and $n_y = 4$.

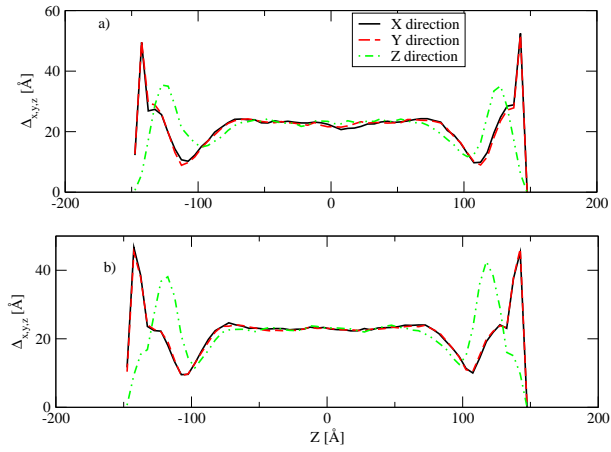


FIG. 9: Average distance of between head to tail of polyelectrolytes with 25 segments for component in x, y directions for a) $n_x = n_y = 3$ and b) $n_x = n_y = 3$.

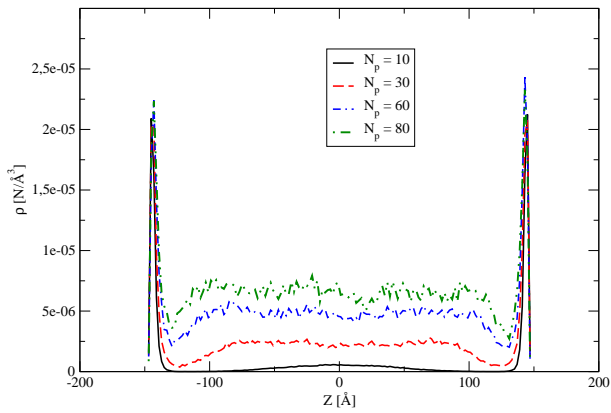


FIG. 10: Density profile of center of mass of polyelectrolytes with 10 segments and different concentration inside the cell. $\sigma_0 = 0.1 \text{ C/m}^2$ and $n_x = 1, n_y = 0$

- ¹J.-L. Barrat and F. Joanny, *Advances in Chemical Physics: Polymeric Systems* **94**, 1 (1996).
- ²P. M. Budd, in *Comprehensive Polymer Science and Supplements*, edited by G. Allen and J. C. Bevington (Pergamon, Amsterdam, 1989) pp. 215 – 230.
- ³B. Bolto and J. Gregory, *Water Research* **41**, 2301 (2007).
- ⁴S. Raj, P. Kumar Sharma, and R. Malviya, *Current Smart Materials* **3**, 21 (2018).
- ⁵A. Laschewsky, *Current Opinion in Colloid & Interface Science* **17**, 56 (2012).
- ⁶A. V. Dobrynin, R. H. Colby, and M. Rubinstein, *Macromolecules* **28**, 1859 (1995).
- ⁷J.-M. Y. Carrillo and A. V. Dobrynin, *Macromolecules* **44**, 5798 (2011).
- ⁸Y. Levin, *Reports on progress in physics* **65**, 1577 (2002).
- ⁹A. B. Lowe and C. L. McCormick, *Chemical reviews* **102**, 4177 (2002).
- ¹⁰P. Chodanowski and S. Stoll, *Macromolecules* **34**, 2320 (2001).
- ¹¹M. Muthukumar, *The Journal of chemical physics* **86**, 7230 (1987).
- ¹²M. Aubouy, O. Guiselin, and E. Raphael, *Macromolecules* **29**, 7261 (1996).
- ¹³A. Bakhshandeh, *Chemical Physics* **513**, 195 (2018).
- ¹⁴A. Bakhshandeh, A. P. Dos Santos, and Y. Levin, *Physical review letters* **107**, 107801 (2011).
- ¹⁵F. V. Goeler, , and M. Muthukumar, *The Journal of chemical physics* **100**, 7796 (1994).
- ¹⁶R. R. Netz and J. F. Joanny, *Macromolecules* **32**, 9026 (1999).
- ¹⁷T. Wallin and P. Linse, *Langmuir* **12**, 305 (1996).
- ¹⁸T. Wallin and P. Linse, *The Journal of Physical Chemistry* **100**, 17873 (1996).
- ¹⁹D. W. McQuigg, J. I. Kaplan, and P. L. J. Dubin, *J. Phys. Chem.* **1992**, 96 (1973).
- ²⁰T. Wallin and P. Linse, *The Journal of Physical Chemistry B* **101**, 5506 (1997).
- ²¹A. P. dos Santos, M. Girotto, and Y. Levin, *The Journal of Physical Chemistry B* **120**, 10387 (2016).
- ²²J. McNamara, C. Kong, and M. Muthukumar, *The Journal of chemical physics* **117**, 5354 (2002).
- ²³M. Muthukumar, *The Journal of chemical physics* **103**, 4723 (1995).
- ²⁴M. Muthukumar, *Proceedings of the National Academy of Sciences* **96**, 11690 (1999).
- ²⁵Y. S. Velichko, F. J. Solis, and M. O. de la Cruz, *The Journal of chemical physics* **128**, 144706 (2008).
- ²⁶M. Seul and D. Andelman, *Science* **267**, 476 (1995).
- ²⁷R. Parthasarathy, P. A. Cripe, and J. T. Groves, *Physical review letters* **95**, 048101 (2005).
- ²⁸R. D. Piner, J. Zhu, F. Xu, S. Hong, and C. A. Mirkin, *science* **283**, 661 (1999).
- ²⁹A. Bakhshandeh, A. P. dos Santos, A. Diehl, and Y. Levin, *The Journal of chemical physics* **142**, 194707 (2015).
- ³⁰A. Bakhshandeh, A. P. dos Santos, and Y. Levin, *Soft Matter* **14**, 4081 (2018).
- ³¹I.-C. Yeh and M. L. Berkowitz, *The Journal of chemical physics* **111**, 3155 (1999).
- ³²A. Bakhshandeh, A. P. dos Santos, A. Diehl, and Y. Levin, *The Journal of Chemical Physics* **151**, 084101 (2019).
- ³³B. Smith and D. Frenkel, *Understanding molecular simulations* (Academic, New York, 1996).
- ³⁴M. P. Allen and D. J. Tildesley, *Computer Simulation of Liquids* (Oxford: Oxford Univ. Press, 1987).